Small Macrocycles As Highly Active Integrin α2β1 Antagonists

Nis Halland,* Horst Blum, Christian Buning, Markus Kohlmann, and Andreas Lindenschmidt

Sanofi R&D, Industriepark Höchst Building G838, D-65926 Frankfurt am Main, Germany

S Supporting Information

ABSTRACT: Starting from clinical candidates Firategrast, Valategrast, and AJM-300, a series of novel macrocyclic platelet collagen receptor α2β1 antagonists were developed. The amino acid derived low molecular weight 14−18-membered macrocycles turned out to be highly active toward integrin α2β1 with IC_{50}s in the low nanomolar range. The conformation of the macrocycles was found to be highly important for the activity, and an X-ray crystal structure was obtained to clarify this. Subsequent docking into the metal-ion-dependent adhesion site (MIDAS) of a β1 unit revealed a binding model indicating key binding features. Macrocycle **38** was selected for further in vitro and in vivo profiling.

KEYWORDS: Integrin, macrocycle, platelet collagen receptor, metathesis, restricted conformation
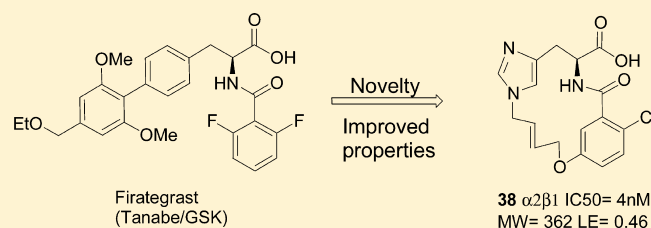
Integrins are a family of adhesion molecules responsible for transmembrane signaling by undergoing conformational rearrangements. They are involved in a wide range of biological processes, e.g., angiogenesis, inflammation, cancer, and hemostasis, and are therefore highly interesting drug targets. Integrins are pairs of noncovalently bound heterodimers, where 18α and 8β units are known to form 24 α/β combinations, making them a functionally and structurally diverse target class.[1−4] We were particularly interested in the biological effects of blocking the integrin α2β1 as this can lead to several therapeutic effects, e.g., antithrombotic[5,6] or antiangiogenic.[7] Our approach toward an orally available small-molecule α2β1 antagonist started with the reported α4β1 (VLA-4) and α4β7 dual antagonists Firategrast,[8] Valategrast,[9] and AJM-300[10] since analogues of these compounds exhibit high activities toward platelet collagen receptor α2β1 (in-house data). As shown in Figure 1, these compounds contain a common L-phenylalanine-N-aroyl motif where the carboxylic acid is responsible for binding to the metal ion in the metal-ion-dependent adhesion site (MIDAS).[11] In order to obtain novel compounds in this highly competitive field we decided to prepare macrocyclic analogues of Firategrast and Valategrast and test them for integrin α2β1 activity. Our strategy was to prepare small macrocycles by using O-allylated L-tyrosine analogues and benzoic acids and subjecting them to ring closing metathesis conditions as this should afford 14−18-membered macrocycles in a highly efficient way in a limited number of steps. Furthermore, the planned macrocycles were expected to have a considerable structural rigidity, improved physicochemical properties, and be Lipinski rule-of-five compatible and thus possibly allowing for oral application.[12] The 6−7 step synthetic route to the macrocycles is exemplified by the synthesis of compounds **6** and **7** in Scheme 1. First, the commercially available N-Boc protected and O-allylated (s)-tyrosine isomer was deprotected and esterified in one pot to
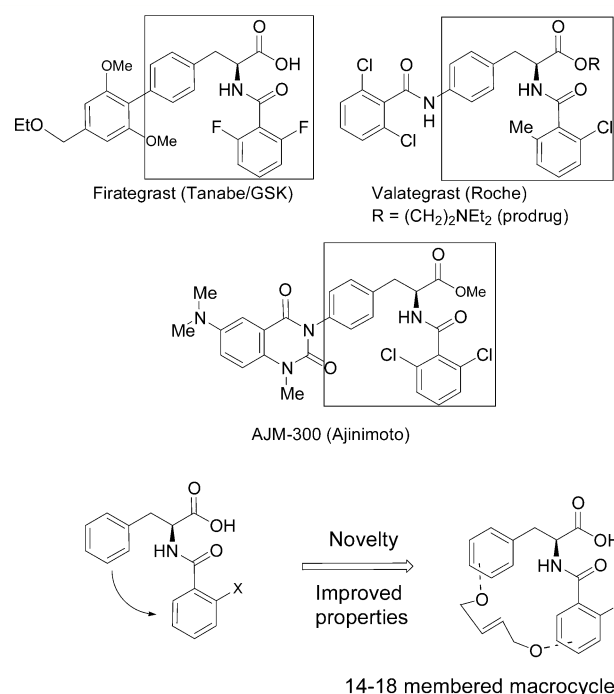

Figure 1. Clinical candidates Firategrast (MS, asthma, and Crohns disease) and Valategrast (MS, RA, and asthma), both discontinued, and AJM-300 (phase II, ulcerative colitis).

afford **1** in 88% isolated yield. The unprotected 2-chloro-5-hydroxybenzoic acid was selectively allylated in 76% yield with

Scheme 1. General Synthetic Route to Macrocycles As Exemplified by the Synthesis of 6 and 7[a]
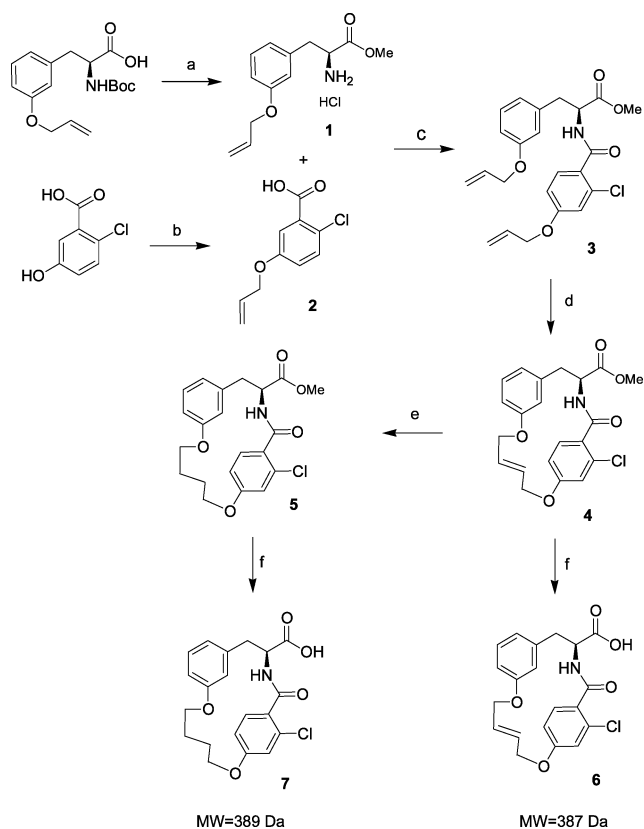
[a]Reactions and conditions: (a) AcCl, MeOH, reflux, 88%. (b) Allylbromide, Bu$_4$POH (40% aq), THF, rt, 76%. (c) HOBt, EDC, DIPEA, DMF, rt, 72%. (d) Hoveyda–Grubbs second generation catalyst, DCM, reflux, 3 h, 87%. (e) PtO$_2$, H$_2$ (1 bar), THF-MeOH, rt, 99%. (f) NaOH, THF–water, rt, 20 h, 78%.

allylbromide using tetrabutylphosphonium hydroxide as the base.[13]

The two allylated fragments were condensed using standard peptide coupling procedures to obtain the precursor **3** for the ring closing metathesis step. After screening a number of catalysts it was found that the relatively stable second generation Hoveyda–Grubbs catalyst in refluxing CH$_2$Cl$_2$ afforded the cyclized metathesis product **4** in 87% yield when the concentration was kept below 2 mM. The cis/trans selectivity was very high as expected, favoring formation of the trans double bond. Hydrolysis of the methyl ester provided the unsaturated macrocyclic carboxylic acid **6**.

The saturated macrocyclic carboxylic acid **7** was obtained by reducing the alkene with hydrogen (1 bar) and a PtO$_2$ or Rh/C catalyst after the ring closing metathesis step. The macrocycles **6** and **7** were tested in a collagen-interaction solid phase assay, mimicking the adhesion of $\alpha2\beta1$-expressing cells with the ECM, for activity on integrin $\alpha2\beta1$. The recombinantly expressed extracellular part of the collagen-binding integrin $\alpha2\beta1$, was coated to 96-well plates and incubated with biotinylated collagen in the presence or absence of serial dilutions of the macrocycles.[14] The readout was via a peroxidase reaction with the substrate ABTS. The absorbance was determined in a microplate reader at 405 nm. The percentage of inhibition of the macrocycles was calculated and reported as IC$_{50}$ values (μM).

To our delight, the tested macrocycles showed high activities of IC$_{50}$ = 163 and 114 nM, respectively. This encouraged us to prepare regioisomeric macrocycles **8**−**16** using the same synthetic route. As shown in Table 1, attaching the linker at

## Table 1. SAR of Macrocyclic Hydroxyphenylalanines/Tyrosine Regioisomers 6−16

compd	phenylalanine linker pos.	benzamide linker pos.	alkene/ saturated	IC$_{50}$ (μM)
valategrast–OH				0.214
6	3	4	alkene	0.163
7	3	4	saturated	0.114
8	3	3	alkene	0.233
9	3	3	saturated	0.142
10	3	2	alkene	0.588
11	3	2	saturated	0.978
12[a]	2	3	saturated	>4
13	4	2	alkene	0.178
14	4	2	saturated	0.106
15	4	3	alkene	0.101
16	4	3	saturated	0.731

[a]Racemic compound.

the meta position of the phenylalanine and the other end to the 3 or 4 position of the benzamide afforded highly active macrocyclic integrin $\alpha2\beta1$ antagonists (compounds **6**−**9**) with activities in the IC$_{50}$ = 100−200 nM range. Attachment to the benzamide 2 position afforded somewhat less active compounds (compounds **10**, **11**), but activity was regained by moving the linker from the meta position to the para position of the phenylalanine/tyrosine (macrocycles **13**−**16**), and compound **15** was found to be the most active macrocycle with an activity on $\alpha2\beta1$ of IC$_{50}$ = 101 nM.

The nature of the linker, n-butyl or 2-butenyl, seemed only to have a minor effect on the $\alpha2\beta1$ activity in most macrocycles, except for the pair **15** and **16**, where a 7-fold decrease in activity was observed upon saturating the linker. It has previously been reported that at least one ortho substituent is required on the benzamide moiety in order to obtain activity on integrins $\alpha4\beta1$ and $\alpha4\beta7$ as the substituent twists the conformation of the amide out of the plane and thus structurally mimics the natural RGD peptide substrates.[9,15,16] This turned out to be true for integrin $\alpha2\beta1$ as well, as all attempts to replace the chlorine atom in the 6-position afforded much less active compounds as shown in Table 2. Replacing the chlorine atom with smaller substituents, e.g., a hydrogen or fluorine atom as in Firategrast afforded poorly active compounds with IC$_{50}$ > 1 μM (compounds **17**, **20**−**23**). Methyl substitution as in Valategrast afforded moderately active macrocycles **18** and **19** that were 3−7 times less potent than their corresponding chloro substituted analogues **8** and **9**. The 6-nitro substituted macrocycle **25** afforded a moderate activity of IC$_{50}$ = 667 nM, whereas the 6-methoxy substituted macrocycle **24** and the CF$_3$-substituted nicotinamide **26** were only weakly active. Because of the unsuccessful attempt to introduce other substituents all further

Table 2. Replacement of 6-Chloro Substituent in Meta-Linked Phenylalanines
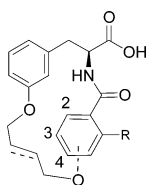
compd	R	benzamide linker pos.	alkene/saturated	IC$_{50}$ (μM)
17	H	3	saturated	>10
18	Me	3	saturated	0.745
19	Me	3	alkene	1.05
20	F	4	alkene	>1
21	F	4	saturated	>4
22	F	2	alkene	>1
23	F	2	saturated	>1
24	OMe	2	saturated	>4
25	NO$_2$	3	saturated	0.667
26[a]	CF$_3$	4	alkene	1.9

[a]Nicotinamide (N in 3-position) was used instead of benzamide.

macrocycles were prepared with a 6-chloro substituent on the benzamide moiety. We then focused on reducing lipophilicity and plasma protein binding by replacing the phenylalanine with other amino acids carrying heteroaromatic rings such as tryptophan or histidine as well as synthetic amino acids.

The macrocycles **29–39** were synthesized according to the general synthetic route described in Scheme 1, and their structure and $\alpha 2\beta 1$ inhibitory activity is shown in Table 3. The novel 1,2,3-triazole α-amino acids used in the synthesis of macrocycles **34–37** were prepared using click chemistry (Scheme 2).

By linking directly through the 5-membered heterocycle, the ring size is reduced by one oxygen atom and thereby changing the conformation of the macrocycle, possibly explaining the increased activity. This positive effect was confirmed by the macrocycles **34** and **36** having an 1,2,3-triazole α-amino acid and an alkene linker displayed activities of IC$_{50}$ = 38 and 34 nM, respectively. Interestingly, the unreduced 2-butenyl linkers generally displayed superior activities of more than a factor 10 compared to the corresponding *n*-butyl linkers when attached to a heteroaromatic amino acid, a trend that is not obvious for macrocycles **6–16** (Table 1). Replacing the phenyl group with 2-aminopyridine as in compounds **29** and **30** only afforded poor $\alpha 2\beta 1$ inhibitors, whereas replacement with a pyridine as in compounds **31** and **32** yielded similar activities compared to macrocycles **15** and **16** (Table 1). Using tryptophan, linked through the indole nitrogen, instead of phenylalanines afforded the very potent $\alpha 2\beta 1$ inhibitor **33** with an IC$_{50}$ = 12 nM. This result demonstrated that a highly active macrocycle conformation could be achieved when a 1,3-substituted 5-membered heteroaromatic ring was used instead of a 6-membered (hetero)aromatic ring.

This illustrates that even small conformational changes can lead to large changes in inhibitory activity toward integrin $\alpha 2\beta 1$. We also prepared histidine derived macrocycles employing a novel $N(\tau)$ selective allylation procedure to afford protected $N(\tau)$-allyl histidine as the starting material.[17] This provided us with our so far most active macrocycle **38** having an IC$_{50}$ = 4 nM, a molecular weight of 362 Da, and a very good ligand efficiency of LE = 0.46 kcal/mol. As histidine has a

Table 3. Heteroaromatic Replacement of Phenyl in Phenylalanine
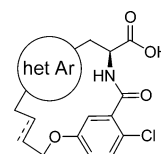
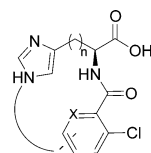| compound	Het Ar	Alkene/ saturated	Macrocycle size	IC$_{50}$ (μM)
29		alkene	16	>1
30		saturated	16	>1
31		alkene	17	0.134
32		saturated	17	0.792
33		alkene	15	0.012
34[a]		alkene	15	0.038
35		saturated	15	1.297
36		alkene	15	0.034
37		saturated	15	0.497
38		alkene	15	0.004
39		saturated	15	0.366

[a]$E/Z \approx 3{:}1$.

Scheme 2. Synthesis of Novel 1,2,3-Triazole α-Amino Acids[a]
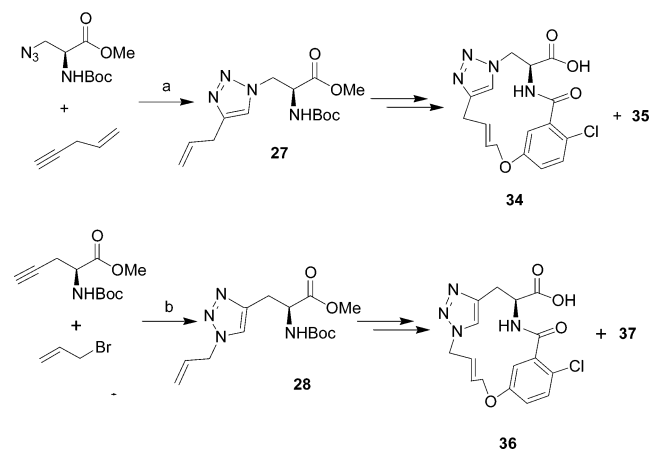
[a]Reactions and conditions: (a) CuSO$_4$, L-ascorbic acid sodium salt, *t*BuOH–water, rt, 79%. (b) NaN$_3$, CuSO$_4$, L-ascorbic acid sodium salt, *t*BuOH–water, rt, 13% (regioisomer **28**).

tendency to racemize, the optical purity of **38** was determined by chiral stationary phase HPLC to be >95% and thus not compromised during preparation. We decided to expand the series of histidine derived macrocycles by making various analogues as depicted in Table 4.

Attaching the linker to the benzamide 4-position as in compound **40** (IC$_{50}$ = 470 nM) and thereby expanding the macrocycle to a 16-membered ring led to a >100-fold loss of activity compared to the 3-substituted regioisomer **38**. As expected, macrocycles prepared from D-histidine, D-**38** and D-

Table 4. Histidine Derived Heterocycles

compd	X	n	linker	macrocycle size	IC$_{50}$ (μM)
40	CH	1	4-OCH$_2$(CH)$_2$CH$_2$	16	0.470
D-**38**	CH	1	3-OCH$_2$(CH)$_2$CH$_2$	15	0.909
D-**39**	CH	1	3-O(CH$_2$)$_4$	15	>4
41	CCl	1	3-OCH$_2$(CH)$_2$CH$_2$	15	0.869
42	N	1	3-OCH$_2$(CH)$_2$CH$_2$	15	0.036
43[a]	CH	1	3-OCH$_2$(CH)$_2$CH$_2$	15	>4
44[b]	CH	2	3-OCH$_2$(CH)$_2$CH$_2$	16	>5
45[b]	CH	2	3-O(CH$_2$)$_4$	16	>5
46[c]	CH	1	3-OCH$_2$(CH)$_2$(CH$_2$)$_2$	16	0.270
47	CH	1	3-O(CH$_2$)$_5$	16	0.731
48	CH	1	3-CH$_2$(CH)$_2$CH$_2$	14	0.176

[a]5-Chlorohistidine. [b]Racemic homohistidine. [c]E/Z $\approx$ 3:1.

39, exhibited decreased activities compared to macrocycles synthesized using L-histidine. Adding a second *ortho*-chloro substituent to the benzamide moiety as in AJM-300 also led to a strong decrease in activity with **41** having an IC$_{50}$ = 869 nM. However, picolinic acid derived macrocycle **42** having a nitrogen atom in the same position displayed an excellent activity of IC$_{50}$ = 36 nM. We also attempted some modifications on the histidine part of the molecule by introducing a chlorine atom in the 5-position of the histidine ring **43** or enlarging the ring by using homohistidine **44** and **45**, but these efforts only yielded inactive compounds. On the contrary, expanding the macrocycle to a 16-membered ring by increasing the length of the linker between the histidine and the benzamide moiety still delivered active compounds **46** and **47** with IC$_{50}$ = 270 and 731 nM, respectively. Contracting the ring to a 14-membered heterocycle by removing the oxygen atom in the linker also led to a decrease in activity with **48** having an activity of IC$_{50}$ = 176 nM. Unfortunately, none of the modified histidine containing macrocycles in Table 4 were superior to macrocycle **38**, and we therefore decided to focus our further profiling on this macrocycle. Since it was obvious that even small conformational changes in the macrocycles could have dramatic effects on integrin $\alpha2\beta1$ activity, we attempted to obtain an X-ray crystal structure of compound **38** to determine the exact configuration of the compound. This was unsuccessful but high quality crystals were obtained by recrystallizing the TFA salt of the cyclopropylmethylester **49** from ethanol−water (Figure 2).[18] This revealed a rigid stair-like structure with an *E*-alkene linker and a benzamide that is twisted 116° out of the plane.

The classification of the torsion angle has been done in the context of published X-ray structures available in the CSD database. The statistical distribution of benzamide torsion angles from representative molecules is depicted in Figure 3. Obviously, the amide torsion angle of macrocycle **49** falls into a sparsely populated region emphasizing its exceptional geometry and a comparable analysis of ortho-substituted benzamides leads to the same conclusion (see Supporting Information). Previously, an exhaustive investigation of fragment geometries in the PDB and CSD from Stahl et al. already indicated this observation for the benzamide torsion angle.[19] It is likely that
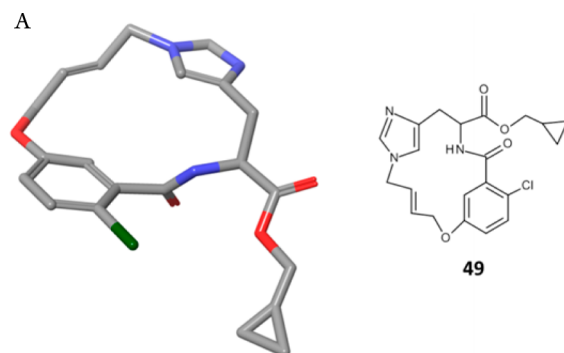
A

Figure 2. (A) X-ray structure of compound **49**. TFA salt, ethanol, and water removed for clarity.
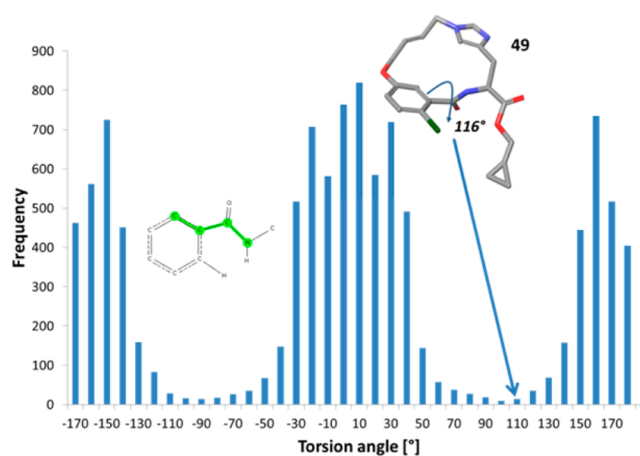

Figure 3. Histogram of the torsion angle distribution of the amide bond in the benzamide fragment as depicted on the basis of an analysis of the CSD.

the twisted amide conformation, facilitated by the ortho-substituent, is required for obtaining activity on integrin $\alpha2\beta1$ as this is very sensitive to the nature of the substituent as demonstrated by the compounds in Table 2. A twisted benzamide conformation of 87° is also observed in a Valategrast intermediate and thus also seems to be required for integrin $\alpha4\beta1$ and $\alpha4\beta7$ binding.[9] To rationalize this observation, a docking model of **38** to the extracellular domain (ECD) of $\alpha5\beta1$ was generated as depicted in Figure 4.

The coordinates from the X-ray structure of **49** have been used as the starting geometry for a docking study for compound **38**. Generally, compound **38** shows high activity on $\alpha2\beta1$ (IC$_{50}$ = 4 nM) as well as on $\alpha5\beta1$ (IC$_{50}$ = 74 nM) (see Table 5). Additionally, due to highly conserved $\beta1$ subunits, $\alpha5\beta1$ is a valid surrogate for $\alpha2\beta1$. The coordinates for the $\alpha5\beta1$ ECD were taken from the PDB entry 3vi4.[20] GLIDE XP (Schrödinger Inc.) was used for the docking studies.[21] The docking mode of **38** in $\alpha5\beta1$ indicates that the carboxylic acid of **38** binds to the buried Mg^{2+} ion in the MIDAS in the $\beta1$ domain. The macrocycle is rigidly fixed to the MIDAS by H-bond interactions from the carboxylate group and the amide of **38** to the $\beta1$ subunit backbone amino acids ASN224 and TYR133. Furthermore, the N3 nitrogen of the imidazole forms a weak H-bond interaction with the hydroxyl group of SER227. Interestingly, only due to the unusual amide geometry of the benzamide torsion the 6-chloro substituent is in a position to fit into a small lipophilic pocket in close proximity to the Mg^{2+} ion completing the binding pharmacophore of **38**. This observation
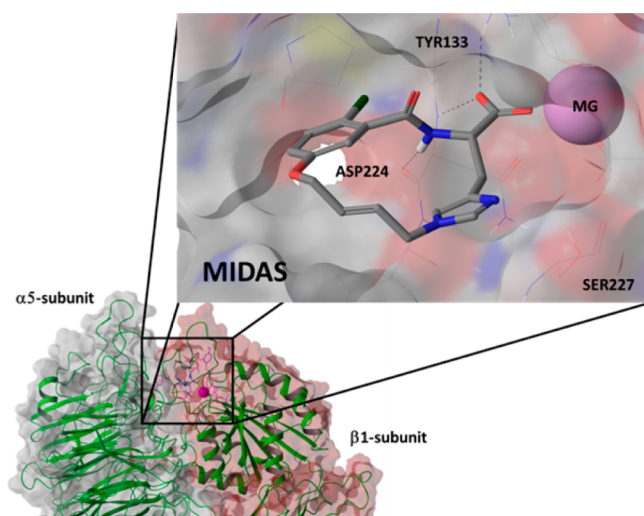
Figure 4. Docking model of the binding of **38** to the MIDAS of $\alpha 5\beta 1$. The van der Waals surface is shown for the extracellular domain of $\alpha 5\beta 1$ ($\alpha 5$, gray; $\beta 1$, pink). The MIDAS is shown as a close-up including the van der Waals surface and the docked ligand in capped sticks. The coloring of the surface is by element. Hydrogen bonds are displayed as dotted lines. The Mg^{2+} ion is depicted as a pink sphere (MG).

Table 5. Physicochemical, in Vitro, and ADMET Properties of 38

38
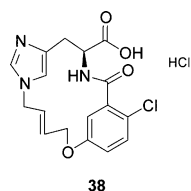
MW	362 (parent)
ligand efficacy	0.46
LogD (pH 7.4, 25 °C)	0.05
CLogP	1.9
PSA (Å^2)	93.5
H-bond donors	2
H-bond acceptors	7
rotatable bonds	1
IC$_{50}$ $\alpha 2\beta 1$	4 nM
IC$_{50}$ $\alpha 1\beta 1$	33 nM
IC$_{50}$ $\alpha 5\beta 1$	74 nM
solubility (pH =7.4, 25 °C)	1.54 mg/mL
metabolic lability in human microsomes	3% (low)
metabolic lability in rat microsomes	0%
metabolic lability in mouse microsomes	0%
plasma stability (human, mouse, and rat)^a	stable
Caco2 permeability ($\times$ 10^{-7}cm/s)	1 (low)
CYP3A4 inhibition IC$_{50}$^{b}	>30 μM
CYP1A1, CYP1A2, and CYP3A4 induction	<10%
hERG channel inhibition IC$_{50}$^{c}	>10 μM

^{a}The compound was spiked to each of the blank plasmas at a concentration of 100 ng/mL. The spiked plasma samples were incubated in a water bath at 37 °C for up to 4 h. ^{b}Incubated at 37 °C for 10−30 min at 0.3−30 μM.[22] ^{c}Patch-clamp technique in the whole-cell configuration on recombinant chinese hamster ovary (CHO) cells.

is in line with the SAR of the 6-chloro substituent in meta linked phenylalanines as discussed earlier (Table 2) and might

explain the fact that the lack of a substituent in this position leads to weakly active compounds.

The hydrochloride salt of macrocycle **38** was selected for further in vitro profiling in order to assess its properties and potential as preclinical candidate, and the results are presented in Table 5. As expected, **38** also showed high activity toward integrins $\alpha 1\beta 1$ and $\alpha 5\beta 1$ with an IC$_{50}$ = 33 and 74 nM, respectively in ELISA-based protein−protein interaction assays. The compound was found to be very polar with a LogD = 0.05 and therefore possessed an excellent solubility of 1.54 mg/mL. Furthermore, it was completely stable when incubated with human, mouse, or rat microsomes or in plasma. Unfortunately, the Caco-2 permeability of **38** was practically nonexistent with a value of 1 $\times$ 10^{-7}cm/s, but methyl, ethyl, and other ester prodrugs displayed a high Caco-2 permeability (>20 $\times$ 10^{-7}cm/s) although they were found to hydrolyze to some extent under the assay conditions.

Furthermore, compound **38** was found to have no inhibitory activity neither on the hERG channel nor on cytochrome P450 CYP3A4 as well as no relevant induction effects on isozymes CYP1A1, CYP1A2, CYP3A4. Because of this promising in vitro profile, compound **38** was further profiled in an in vivo pharmacokinetic study in rat to determine important pharmacokinetic parameters. After intravenous bolus administration of 4.8 mg/kg, blood and urine samples were collected for up to 24 h, and the key pharmacokinetic parameters are shown in Table 6. It was found that 24% of the administered

Table 6. Pharmacokinetic Parameters in Rat after Intravenous Bolus Administration of 4.8 mg/kg

$t_{1/2}$ (hr)	0.24
C_0 (μg/mL)	1.7
V_{ss} (L/kg)	3.6
% of dose excreted into urine (24 h)	24
% of dose excreted into bile (2 h)	50

dose of compound **38** was excreted unchanged into the urine after 24 h, and in an additional study, approximately 50% was going unchanged into bile after 2 h. This resulted in a very short half-life of approximately 15 min and plasma level <10 ng/mL 1 h after administration. The PK profile was found to be unacceptable due to the very short half-life and extensive excretion and no further studies were performed on compound **38**.

In conclusion, we have developed highly active low molecular weight macrocyclic integrin $\alpha 2\beta 1$ antagonists from acyclic precursors. These small macrocycles constitute a novel class of integrin inhibitors with improved and attractive properties such as high solubility and metabolic and plasma stability in human, mouse, and rat. Unfortunately the compounds exhibited poor cellular permeability and were extensively cleared from plasma and thus exhibited a very short half-life in vivo.

■ ASSOCIATED CONTENT

Ⓢ Supporting Information

Representative experimental procedures for synthesis of macrocycles, biochemical assays, and analytical data. This material is available free of charge via the Internet at http://pubs.acs.org.

AUTHOR INFORMATION

Corresponding Author

*(N.H.) Phone: +49-69305-36193. E-mail: nis.halland@sanofi.com.

Notes

The authors declare no competing financial interest.

REFERENCES

(1) Hynes, R. O. Integrins: Bidirectional allosteric signaling machines. *Cell* **2002**, *110*, 673−687.

(2) Shimaoka, M.; Springer, T. A. Therapeutic antagonists and conformational regulation of integrin function. *Nat. Rev. Drug Discovery* **2003**, *2*, 703−716.

(3) Desgrosellier, J. S.; Cheresh, D. A. Integrins in cancer: biological implications and therapeutic opportunities. *Nat. Rev. Cancer* **2010**, *10*, 9−22.

(4) Cox, D.; Brennan, M.; Moran, N. Integrins as therapeutic targets: lessons and opportunities. *Nat. Rev. Drug Discovery* **2010**, *9*, 804−820.

(5) Miller, M. W.; Basra, S.; Kulp, D. W.; Billings, P. C.; Choi, S.; Beavers, M. P.; McCarty, O. J. T.; Zou, Z.; Kahn, M. K.; Bennet, J. S.; DeGrado, W. F. Small-molecule inhibitors of integrin α2β1 that prevent pathological thrombus formation via an allosteric mechanism. *Proc. Natl. Acad. Sci. U.S.A.* **2009**, *106*, 719−724.

(6) Nuyttens, B. P.; Thijs, T.; Deckmyn, H.; Broos, K. Platelet adhesion to collagen. *Thrombosis Res.* **2011**, *127* (suppl 2), S26−29.

(7) San Antonio, J. D.; Zoeller, J. J.; Habursky, K.; Turner, K.; Pimtong, W.; Burrows, M.; Choi, S.; Basra, S.; Bennet, J. S.; DeGrado, W. F.; Iozzo, R. V. A key role for the integrin α2β1 in experimental and developmental angiogenesis. *Am. J. Pathol.* **2009**, *175*, 1338−1347.

(8) Kawaguchi, T.; Nomura, S.; Tsukimoto, M.; Kume, T. Sircar, I. Inhibitors of α4 mediated cell adhesion. WO200218320, 2001.

(9) Sidduri, A.; Tilley, J. W.; Lou, J. P.; Chen, L.; Kaplan, G.; Mennona, F.; Campbell, R.; Guthrie, R.; Huang, T.-N.; Rowan, K.; Schwinge, V.; Renzetti, L. M. N-Aroyl-l-phenylalanine derivatives as VCAM/VLA-4 antagonists. *Bioorg. Med. Chem. Lett.* **2002**, *12*, 2479−2482.

(10) Thomson Reuters Cortellis database.

(11) Heckmann, D.; Laufer, B.; Marinelli, L.; Limongelli, V.; Novellino, E.; Zahn, G.; Stragies, R.; Kessler, H. Breaking the dogma of the metal-coordinating carboxylate group in integrin ligands: Introducing hydroxamic acidsto the MIDAS to tune potency and selectivity. *Angew. Chem., Int. Ed.* **2009**, *48*, 4436−4440.

(12) Giordanetto, F.; Kihlberg, J. Macrocyclic drugs and clinical candidates; What can medicinal chemists learn from their properties. *J. Med. Chem.* **2013**, DOI: 10.1021/jm400887j.

(13) Liu, P.; Huang, L.; Faul, M. M. A simple method for chemoselective phenol alkylation. *Tetrahedron Lett.* **2007**, *48*, 7380−7382.

(14) Eble, J. A.; Beermann, B.; Hinz, H. J.; Schmitt-Hederich, A. α2β1 Integrin is not recognized by rhodocytin but is the specific, high affinity target of rhodocetin, an RGD-independent disintegrin and potent inhibitor of cell adhesion to collagen. *J. Biol. Chem.* **2001**, *276*, 12274−12284.

(15) Gong, Y.; Barbay, J. K.; Kimball, E. S.; Santulli, R. J.; Fisher, M. C.; Dyatkin, A. B.; Miskowski, T. A.; Hornby, P. J.; He, W. Synthesis and SAR of pyridazinone-substituted phenylalanine amide α4 integrin antagonists. *Bioorg. Med. Chem. Lett.* **2008**, *18*, 1331−1335.

(16) Sircar, I.; Gudmundsson, K. S.; Martin, R.; Liang, J.; Nomura, S.; Jayakumar, H.; Teegarden, B. R.; Nowlin, D. M.; Cardarelli, P. M.; Mah, J. R.; Connel, S.; Griffith, R. C.; Lazarides, E. Synthesis and SAR of N-benzoyl-L-biphenylalanine derivatives: Discovery of TR14035 a dual α4β7/α4β1 integrin antagonist. *Bioorg. Med. Chem.* **2002**, *12*, 2051−2066.

(17) Halland, N. An atom-efficient direct regioselective N(τ)-allylation of histidine derivatives. *Synlett* **2012**, 2969−2971.

(18) The TFA salt of compound **49** was recrystallized from ethanol−water. Crystal size (mm) 0.5 × 0.4 × 0.07. Space group $P2_1/n$. Deposited in the Cambridge crystallographic database under number CCDC 978145.

(19) Grameld, K. A.; Kuhn, B.; Reuter, D. C.; Stahl, M. Small molecule conformational preferences derived from crystal structure data. A medicinal chemistry focused analysis. *J. Chem. Inf. Model.* **2008**, *48*, 1−24.

(20) Nagae, M.; Nogi, T.; Takagi, J. Crystal structure of α5β1 integrin ectodomain: Atomic details of the fibronectin receptor. *J. Cell. Biol.* **2012**, *197* (1), 131−140.

(21) Friesner, R. A.; Murphy, R. B.; Repasky, M. P.; Frye, L. L.; Greenwood, J. R.; Halgren, T. A.; Sanschagrin, P. C.; Mainz, D. T. Extra precision glide: docking and scoring incorporating a model of hydrophobic enclosure for protein−ligand complexes. *J. Med. Chem.* **2006**, *49* (21), 6177−6196.

(22) Dudda, A.; Kürzel, G. U. Drug−Drug Interaction−Enzyme Inhibition. In *Drug Discovery and Evaluation: Safety and Pharmacokinetic Assays*, 1st ed.; Vogel, H. G., Hock, F. J., Maas, J., Mayer, D., Eds.; Springer: New York, 2006; pp 551−557.

198

dx.doi.org/10.1021/ml4004556 | *ACS Med. Chem. Lett.* 2014, 5, 193−198